



**SPAWAR**  
**Systems Center**  
**San Diego**

TECHNICAL REPORT 1808  
November 1999

# **Fiscal Year 1999 Wideband Antenna Feasibility Study**

**Man-Carried Ultrawideband  
Antenna System**

**R. C. Adams**  
**LCDR C. P. Haglind**  
**LCDR (sel.) H. N. Pace, Jr.**  
**SSC San Diego**

**J. Lebaric**  
**R. Adler**  
**CAPT T. M. Gainor**  
**A. T. Tan**  
**Naval Postgraduate School**

Approved for public release;  
distribution is unlimited.

**SSC San Diego**

**19991227 026**

TECHNICAL REPORT 1808  
November 1999

# **Fiscal Year 1999 Wideband Antenna Feasibility Study**

Man-Carried Ultrawideband  
Antenna System

**R. C. Adams**  
**LCDR C. P. Haglind**  
**LCDR (sel.) H. N. Pace, Jr.**  
SSC San Diego

**J. Lebaric**  
**R. Adler**  
**CAPT T. M. Gainor**  
**A. T. Tan**  
Naval Postgraduate School

Approved for public release;  
distribution is unlimited.



SSC San Diego  
San Diego, CA 92152-5001

**SSC SAN DIEGO**  
**San Diego, California 92152-5001**

---

**E. L. Valdes, CAPT, USN**  
**Commanding Officer**

**R. C. Kolb**  
**Executive Director**

**ADMINISTRATIVE INFORMATION**

The work described in this report was performed for the Amphibious Warfare Technology (AWT) Office at Marine Corps Systems Command (MARCORSYSCOM) by the SSC San Diego Signal Processing & Communication Technology Branch (D855).

Released by  
C. R. Hendrickson, Head  
Signal Processing &  
Communication Technology  
Branch

Under authority of  
C. J. Sayre, Head  
Electromagnetics &  
Advanced Technology  
Division

**ACKNOWLEDGMENTS**

We would like to acknowledge the assistance of the following personnel at SSC San Diego. Dam Tam (D856 Branch Head) provided complete cooperation in scheduling the experiments at the Model Range. Rick Nielsen (D851) conducted the experiments to measure the patterns. Robert Abramo (D856) conducted the experiments on the measurement of the impedance and provided valuable expertise during the measurement of the patterns. Robert O. Henry (D856) and Mike McGinnis (D851) assisted in many ways in measuring both patterns and impedance. Robert O'Neill of the Model Shop (PWC 586) fabricated the RF Vest antenna and the Styrofoam model.

## EXECUTIVE SUMMARY

Antennas carried by foot soldiers are typically optimized for a particular type of radio. Often, they have a very small bandwidth and lack convenience. Many of these antennas are whips that extend above the soldier's height and increase vulnerability to detection and the likelihood of ensnaring in low-hanging trees.

The Joint Tactical Radio System (JTRS) provides an opportunity to develop an ultrawideband antenna system that is fully portable and convenient. This system will provide compatibility with all legacy waveforms and current radios and will transmit or receive for any frequency between 2 MHz and 2000 MHz. The antenna system for this radio should be completely integrated into the soldier's uniform.

Researchers at the Naval Postgraduate School determined that several antennas would be needed to cover the full frequency band. An antenna that covers the 30- to 500-MHz band could be fabricated and incorporated into the soldier's vest. A helmet would be the basis for an antenna for the 500- to 2000-MHz band. The overall objective of the FY 1999 effort was to develop models of the RF Vest antenna.

FY 1999 goals were to: (1) conduct a survey of the technical literature to determine what efforts had been undertaken to develop a man-carried ultrawideband antenna, (2) develop theoretical models of several types of antennas, (3) predict the performance of these types, (4) fabricate and test one model for which predictions had been made, (5) evaluate the validity of the models by comparing theory and experiment, and (6) optimize the validated theoretical models to cover an important frequency band. Each of these goals was accomplished.

A literature survey indicates that no technology presently available had the correct combination of portability, polarization, omnidirectionality, and ultrawideband operation. A novel approach is needed.

Theory confirmed by experiment indicates that an antenna in the form of a vest provides efficient operation (voltage standing wave ratio [VSWR] less than 3:1) for 125- to 500-MHz frequencies. The predictions also indicate that a suitable design in the vest fabric will allow efficient operation in the important bands (30 to 88 MHz and 225 to 500 MHz).

The simplest design for which predictions had been made was fabricated and tested at SPAWAR Systems Center, San Diego (SSC San Diego). A Styrofoam model was built as a filling for the vest. Impedance measurements show almost complete agreement between theory and experiment. Both theory and experiment indicate a strong resonance near 100 MHz. The only disagreement between theory and experiment is near the 350-MHz frequency. The likely cause of this disagreement is the feed region that cannot be modeled by the tools at hand.

The presence of a person wearing the vest makes the antenna more efficient at frequencies between 65 MHz and 200 MHz but less efficient at frequencies above 300 MHz.

The agreement between theory and experiment for the azimuth patterns is good for all frequencies. The locations of nulls in the pattern correspond completely. Null depth in the theoretical predictions is somewhat larger for theory compared to experiment.

The agreement between theory and experiment for the elevation patterns is reasonably good for most frequencies as long as the finite conductivity of the ground plane is considered. The agreement is best for frequencies above 200 MHz. For the measurements taken at a frequency of 100 MHz, the antenna is probably not in the far field. Also, there is strong coupling between the ground plane and the vest at 100 MHz.

Copper interwoven with polyester is excellent for use in the RF Vest. This material has high conductivity, good airflow, high flexibility, small weight, and high strength.

# CONTENTS

<b>EXECUTIVE SUMMARY .....</b>	<b>iii</b>
<b>1. INTRODUCTION.....</b>	<b>1</b>
1.1 PROGRAM BACKGROUND.....	1
1.2 SCOPE .....	2
1.3 OPERATIONAL CONCERNS .....	2
1.4 GOALS AND OBJECTIVES .....	2
<b>2. DESIGN APPROACH.....</b>	<b>3</b>
<b>3. RESULTS .....</b>	<b>5</b>
3.1 LITERATURE STUDY .....	5
3.1.1 Books on Frequency Independent Antenna Engineering and Design .....	5
3.1.2 IEEE/IEE Technical Publications .....	5
3.1.3 Books on Small Antennas for Mobile Phones.....	7
3.1.4 Conclusion .....	7
3.2 ANTENNA DESIGN .....	7
3.3 PROTOTYPE CONSTRUCTION.....	8
3.3.1 Material .....	9
3.3.2 Styrofoam Model.....	9
3.3.3 RF Vest Antenna Fabrication.....	10
3.4 PERFORMANCE TEST RESULTS.....	11
3.4.1 Impedance .....	12
3.4.2 Radiation Patterns .....	14
<b>4. THEORY AND EXPERIMENT RESULTS/COMPARISON/ANALYSIS .....</b>	<b>21</b>
4.1 IMPEDANCE .....	21
4.2 RADIATION PATTERNS IN AZIMUTH.....	23
4.3 RADIATION PATTERNS IN ELEVATION .....	25
<b>5. CONCLUSIONS .....</b>	<b>29</b>
<b>6. RECOMMENDATIONS.....</b>	<b>31</b>
6.1 RF VEST ANTENNA OPTIMIZATION .....	31
6.2 HELMET ANTENNA DEVELOPMENT .....	31
6.3 ASSESSMENT OF INTERACTION BETWEEN PERSON AND ANTENNA .....	31
6.4 HF ANTENNA .....	32
6.5 FULL SYSTEM.....	32
<b>7. REFERENCES .....</b>	<b>33</b>
<b>APPENDIX A. TEST PLAN FOR IMPEDANCE AND RADIATION PATTERN MEASUREMENT OF THE RF VEST.....</b>	<b>A-1</b>

## Figures

1. Wire grid model of simple RF Vest antenna. Feed is in back of vest. Shorting is in front .....	8
2. Styrofoam model.....	10
3. RF Vest antenna (front).....	10
4. RF Vest antenna (back) .....	10
5. RF Vest antenna feed region .....	11
6. Real, imaginary, and magnitude impedance of RF Vest antenna on Styrofoam model .....	12
7. Measured impedance of RF Vest antenna at 32 and 44 inches above ground plane .....	13
8. Comparison of measured impedance of RF Vest antenna on Styrofoam model and man .....	14
9. Comparison of measured VSWR of RF Vest antenna with and without transformer.....	14
10. SSC San Diego Pattern Range .....	16
11. RF Vest antenna and Styrofoam model on Pattern Range .....	17
12. Experimentally determined fields from RF Vest antenna versus azimuth for six elevation angles and a 100-MHz frequency .....	18
13. Experimentally determined fields from RF Vest antenna versus azimuth for six elevation angles and frequencies of 200, 300, 400, and 500 MHz .....	18
14. Experimentally determined field with horizontal and vertical polarization versus azimuth at a 100-MHz frequency .....	19
15. Experimentally determined fields with horizontal and vertical polarization versus azimuth for 200-, 300-, 400-, and 500-MHz frequencies. Elevation angle is 5° .....	19
16. Experimentally determined fields versus elevation angle for 100-, 200-, 300-, 400-, and 500-MHz frequencies. Azimuth angle is 0° .....	20
17. Experimentally determined field versus elevation angle at 100- and 500-MHz frequency .....	20
18. Comparison of experimentally and theoretically determined impedance magnitude versus frequency. Antenna height above ground is 32 inches.....	21
19. Ratio of theoretically determined absolute impedance magnitude to that experimentally determined versus frequency of RF Vest antenna.....	22
20. Comparison of theory to experiment for absolute impedance magnitude. RF Vest antenna height above ground plane is 44 inches .....	22
21. Comparison between experimentally determined fields at 5° elevation angle and theoretical predictions for 100-MHz frequency.....	23
22. Comparison between experimentally determined fields at 5° elevation angle and theoretical predictions for 200-MHz frequency.....	24
23. Comparison between experimentally determined fields at 5° elevation angle and theoretical predictions for 300-MHz frequency.....	24
24. Comparison between experimentally determined fields at 5° elevation angle and theoretical predictions for 400-MHz frequency.....	25
25. Comparison between experimentally determined fields at 5° elevation angle and theoretical predictions for 500-MHz frequency.....	25
26. Comparison between experimentally determined fields versus elevation angle and theoretical predictions for 100-MHz frequency and $\phi = 0$ .....	26

27. Comparison between experimentally determined fields versus elevation angle and theoretical predictions for 200-MHz frequency and $\phi = 0$ .....	26
28. Comparison between experimentally determined fields versus elevation angle and theoretical predictions for 300-MHz frequency and $\phi = 0$ .....	27
29. Comparison between experimentally determined fields versus elevation angle and theoretical predictions for 400-MHz frequency and $\phi = 0$ .....	27
30. Comparison between experimentally determined fields versus elevation angle and theoretical predictions for 500-MHz frequency and $\phi = 0$ .....	28

## Tables

1. FLECTRON properties (Product No. 3027-106 from APM) .....	9
--	---



# **1. INTRODUCTION**

The Wideband Antenna Feasibility Study is an ongoing effort originally funded through the Amphibious Warfare Technology (AWT) Office at Marine Corps Systems Command (MARCORSYSCOM). This report gives a technical account of achievements during Fiscal Year 1999 (FY 1999). It describes the technical considerations addressed and the basis upon which the concept and specific designs were chosen. Theoretically derived predictions as well as test results are included with a concluding analysis and recommendations.

The FY 1999 effort explored advanced antenna designs that are flexible enough to support the dynamic bandwidth capabilities of the Joint Tactical Radio System (JTRS), to incorporate selected legacy radio equipment such as the Single Channel Ground and Airborne Radio System (SINCGARS), and to meet United States Marine Corps (USMC) size and weight constraints.

The approach to the challenge was to combine the knowledge and innovation of the Naval Postgraduate School (NPS) with the understanding, practical experience, and facilities of Space and Naval Warfare Systems Center, San Diego (SSC San Diego). This creative mix of skills has been a good combination for unconventional solutions. NPS performed most of the fundamental theoretical work by doing extensive literature surveys, conducting computer simulations, and developing models. SSC San Diego scientists reviewed all designs, gave advice, and fabricated and tested the prototype.

After a dialogue with MARCORSYSCOM, the proposed concept was explored with Combat Wear Integrated (COMWIN) antennas. The guidance was that the most urgent need, an antenna with a frequency coverage from 30 to 500 MHz, should be addressed first. Consequently, the 5-month emphasis in FY 1999 was to investigate, model, simulate, and test a vest-integrated antenna.

The primary goal for FY 1999 was to investigate different designs and validate the different models to gain confidence in the approach (as opposed to designing an effective prototype antenna). This goal was achieved. The comparison between the theoretically derived predictions and the test results of the prototype provided much valuable and encouraging information. Today, we have a good basis for further exploration and implementation of this antenna concept.

## **1.1 PROGRAM BACKGROUND**

Battlefield digitalization, almost an axiom today, will influence many aspects of warfighting. This evolution will significantly affect various technical systems that support soldiers, sailors, and marines, and specifically, communications, with expanded demand for reliability and data rates.

The JTRS is a wideband software-controlled radio system with a frequency coverage from 2 MHz to beyond 2 GHz. Although the long-term system plan is that it shall replace a whole range of legacy systems, the U.S. military will use modern and older technology for awhile. New antenna systems must be developed to support this mix of radios.

The Marine Corps and MARCORSYSCOM determined that no antenna efforts are currently supported within the JTRS program. Therefore, in February–March, SSC San Diego was asked to propose an effort to address antenna systems for the dismounted Marine. SSC San Diego contacted NPS and proposed the united effort that produced this report.

## **1.2 SCOPE**

The FY 1999 effort was limited by constraints on both time and resources. The time was limited to 20 weeks from May until late September. Literature was searched, a model was developed, a prototype was fabricated, and performance measurements were obtained. The theoretical resources were limited to software already on hand. The overall aim was to prepare for the next effort in FY 2000.

## **1.3 OPERATIONAL CONCERNS**

The USMC communications systems that operate within the 30- to 500-MHz frequency range are as follows:

- AN/PRC-119 VHF SINCGARS family of radios
- AN/PRC-113 UHF ground-to-air radio
- Position-location reporting system and enhanced position location reporting system (PLRS/EPLRS)
- AN/PSC-3 (5)/LST-5 UHF satellite radios operating in line-of-sight (LOS) mode

The radio frequency (RF) Vest antenna scheduled for design in FY 2000 will allow each radio system to be operated in the dismounted mode without current multiple antenna systems. A single RF Vest antenna system may replace the two SINCGARS antennas, the three AN/PRC-113 antennas, the PLRS/EPLRS antennas, and the PSC/LST LOS antennas. The individual antennas operate within the frequency range of a specific radio. The vertical monopole (a “whip”) operating as a ground plane against the radio enclosure has been the primary antenna choice for the radios listed above. Whip antenna bandwidth, while sufficient for each individual radio, does not provide the required frequency coverage for the ultrawide-band JTR. The JTR user must maintain a set of whip antennas and switch them depending on the operational frequency. Not only is this inconvenient logistically, it also precludes simultaneous operation over more than a single frequency band. By operating effectively with the listed radio systems, the RF Vest antenna design removes these restrictions.

## **1.4 GOALS AND OBJECTIVES**

The primary FY 1999 goal was to validate the model used for predicting vest antenna impedance and radiation patterns. The comparison between theory and experiment would illuminate prediction limitations. After the model and predictions have been validated, the model can be varied in a systematic way to meet the requirements.

A secondary goal was to evaluate one material that could be used for the antenna. Metalized cloth consisting of copper fiber interwoven with polyester was used for the antenna. This material was effective both for its high conductivity and flexibility. The material is lightweight and allows much airflow.

## 2. DESIGN APPROACH

During FY 1999, the Naval Postgraduate School team selected the COMWIN design approach. The COMWIN approach is based on integration of antennas with the marine combat gear. This approach is driven by the goal to make the marine radio operator indistinguishable from any other combat-equipped marine while providing maximum antenna performance and maintaining safe operator RF absorption levels. Combat wear items that have been identified for antenna integration are:

- Vest
- Helmet

The COMWIN approach using the vest (hereafter referred to as the RF Vest antenna) has several advantages. The required vertical polarization is "natural" to the RF Vest antenna when the operator is in the upright position. Because of the near rotational symmetry of the RF Vest, the radiation pattern should be reasonably omnidirectional in azimuth. The large surface area of the RF Vest allows for a broadband design. Common to any antenna, the RF Vest dimensions limit the efficient operational frequency to frequencies above a certain low-cutoff frequency. Similarly, above some high frequencies, the RF Vest becomes electrically large and the radiation pattern exhibits multiple nulls and lobes. Therefore, the possibility of using two antennas (one being the RF Vest and the other the RF Helmet) was explored. The RF Vest would cover the frequency range below 500 MHz. The RF Helmet would cover the frequency range above 500 MHz. Except for the section on recommendations, this report now discusses only the RF Vest.

To assess antenna performance and compare different designs, the objective measure of antenna quality at a particular frequency has been defined as the overall efficiency:

$$\eta(f) = \eta_{\text{input}}(f) * \eta_{\text{radiation}}(f) * \eta_{\text{beam}}(f).$$

Computer simulation and/or measurements can obtain three constitutive efficiencies. The first, the antenna input efficiency, depends on matching the antenna input impedance to feed line impedance. This efficiency is equal to the fraction of the "incident" power (from the feed line) accepted by the antenna, with the remaining power reflected back to the source. The second, the antenna radiation efficiency, is equal to the fraction of the power radiated by the antenna relative to the feed line power delivered to the antenna. The remaining antenna-accepted power is dissipated into heat in the antenna itself or its immediate surroundings. The third, the antenna beam efficiency, is the fraction of antenna-radiated power that is directed into the "target sector." This is typically defined by solid angle (where recipients of the antenna energy are expected) and at the polarization that the recipients expect. Based on the above, ideal antenna properties could be postulated as our design target:

- Input impedance purely real and equal to the feed line impedance (at all frequencies of interest)
- No antenna internal losses
- Radiation pattern uniform over the "target" sector and zero elsewhere
- Polarization matched to the "target"

The comparison of different antennas requires that computer simulation or measurements obtain their overall efficiencies. Upon consultation with MARCORSYSCOM, we have assumed the following:

- 50- $\Omega$  feed-line characteristic impedance
  - Vertical polarization
  - Target sector 360° in azimuth (omnidirectional) and 0 to 60° in elevation.
- These goals will be used for antenna performance evaluations and antenna comparisons.

### 3. RESULTS

Results deal with four areas of investigation: (1) a literature survey to reveal other approaches, (2) theoretical model development, (3) prototype fabrication, and (4) measurement of impedance and radiation pattern performance.

#### 3.1 LITERATURE STUDY

The literature survey was conducted for the JTRS antenna (30- to 500-MHz frequency band) and covered the following main categories:

1. Books on frequency-independent antenna engineering and design
2. Technical publications
3. Books on small antennas for cell phones

##### 3.1.1 Books on Frequency-Independent Antenna Engineering and Design

These books provide the general design requirements to achieve frequency independence, which implies wideband antenna operation. In theory, an antenna will be frequency independent if its shape is determined entirely by angles, i.e., its shape does not change under a change of scale (Rumsey, 1966). This property is also known as self-similarity. In practice, there are two other requirements:

- Current on the structure should diminish to zero with distance away from the antenna input terminals (Rumsey, 1966)
- Radiation pattern should not vary with frequency (Rumsey, 1966)

Examples of such antennas are planar spirals, conical spirals, and log-periodic antennas. These antennas are not well-suited for the JTR application because they do not have omnidirectional azimuth radiation patterns, one of the basic requirements.

##### 3.1.2 IEEE/IEE Technical Publications

**3.1.2.1 Fractal Antennas.** Self-similarity is also a property of fractals. Antenna arrays that have fractal geometry could be expected to exhibit frequency-independent behavior (Werner and Werner, 1996). In practice, array antennas designed using fractal structure exhibit multiband instead of frequency-independent behavior (Puente-Baliarda and Pous, 1996).

**3.1.2.2 Antenna Systems.** The search on the IEEE/IEE Online Library yielded two relevant papers on previous efforts to design antenna systems that covered 2 MHz to 3000 MHz:

- Multimode multiband antenna for the Speakeasy Multimode Multiband digital radio
- Spiral-Mode Microstrip (SMM) antenna

**3.1.2.2.1 Speakeasy Multimode Multiband Antenna (Strugatsky and Walter, 1992).** Three teams participated in studies to design an antenna system that covered the 2- to 3000-MHz band. Teams for the different frequency bands summarized the proposals as follows:

### **Team 1 - ITT/University of Illinois/RM Associates**

The HF (2 to 30 MHz) band antenna could be implemented as an end-loaded  $\Gamma$  antenna having full instantaneous bandwidth without a tuning circuit, but with low efficiency.

The VHF/UHF (30 to 1225 MHz) band antenna could be implemented by multiband monopole but not as a full broadband antenna. The length was 1.75 m. Six LC circuits loaded the antenna. The four bands were 30 to 88 MHz, 108 to 152 MHz, 225 to 400 MHz, and 960 to 1225 MHz.

The Wide-angled Stacked Conical Monopole could be considered where a flat mounting surface was available to reduce the antenna profile and size and increase operating bandwidth.

### **Team 2 - GS, Inc.**

The HF band antenna could be implemented by an 18-ft tunable helix.

The VHF band antenna could be implemented by a 20-ft narrowband, multi-turn helix tuned by pin diodes.

### **Team 3 - TRW**

Loop antennas had only a 1-octave bandwidth.

The HF band antenna could be covered by a multiturn loop.

The VHF/UHF antenna could be implemented by a one and a half-turn loop over a ground plane.

Spiral antennas with two arms fed in-phase gave a monopole-type pattern with null on the boresight. The multiarm spiral was viable for a frequency above 300 MHz. The upper limit was approximately 40 GHz. The lower limit was determined by the size of the platform. The lower limit on frequency was inversely proportional to the platform's size.

The broadband monopole antenna was a variant of a discone antenna and consisted of spiral arms.

#### **Number of antennas required:**

Coverage of the 300- to 3000-MHz band required one four-arm spiral or a broadband monopole.

The 108- to 152-MHz and 225- to 400-MHz band required two one-turn loops.

The 30- to 88-MHz band antenna required three two-turn loops.

The 2- to 30-MHz band antenna required three to four multiturn loops.

The manpack required a 9-ft whip or a five-turn multiturn loop with a 12-inch whip extension of one of the turns.

The paper concluded that a viable solution (good electrical performance and low profile) was not found.

**3.1.2.2.2 Spiral-Mode Microstrip (SMM) Antenna (Tripp, 1995).** The Spiral-Mode Microstrip (SMM) antenna was designed using frequency-independent radiating elements (spirals). The antenna was designed for the United States Air Force to operate with the following equipment:

GPS:	1220 to 1580 MHz
JTIDS:	960 to 1215 MHz
IFF:	1030 to 1090 MHz
UHF Communications:	225 to 400 MHz
UHF SATCOM :	240 to 320 MHz

The SMM antenna is a four-arm spiral antenna with a 24-inch diameter (approximately 60 cm) over a ground plane. If mounted vertically, mode zero is a broadside pattern providing good hemispherical coverage in azimuth. The higher modes all have a null on the broadside. The SMM antenna was circularly polarized as the theory predicted. The antenna is impractical for man-portable applications because of its size, requirement of a ground plane, and hemispherical coverage.

### **3.1.3 Books on Small Antennas for Mobile Phones**

The literature on mobile phones did not offer any possible solutions because the emphasis was on antennas designed for commercial operation with a fixed operating frequency rather than for the instantaneous wideband operation of the JTRS. The bandwidth was generally about 10 percent of the operating frequency (Dilworth, 1994; Fujimoto and James, 1994; Fujimoto et al., 1997).

### **3.1.4 Conclusion**

The literature survey did not provide any antenna design that could completely meet JTRS requirements. The conventional self-similar antennas could not be used for the project since such antennas are usually circularly polarized. Vertically polarized antennas would lose half the power in reception. A man-carried antenna that is efficient in the required frequency bands requires a novel approach.

## **3.2 ANTENNA DESIGN**

The RF Vest design was driven by the need to obtain wideband operation with minimum complexity, weight, and cost. The special concern was to obtain the lowest possible operational frequency out of a limited physical size. The basic design selected can be considered as an unconventional combination of a dipole antenna and a loop antenna. The RF Vest (shown in figure 1 as the Mark 1 wire grid model that was used as the basis for the fabricated antenna and measured at SSC San Diego) consists of two metallized cloth parts of approximately equal surface area. Area equalization maximizes the bandwidth.

The two "cylinders" with an approximately elliptical cross section can be considered as elements of the unconventional "dipole" antenna. The RF Vest is fed in the back (where the radio is located) across the gap between the two cylinders. Because the circumference of the cylinders is commensurate with their length, the current follows not only longitudinal paths along the cylinders but also circumferential paths around the cylinders. The perimeter of the gap and a shorting strap opposite to the feed form a loop-like path for the antenna current.

The other surfaces of the two cylinders form the unconventional dipole antenna. If it were not for the shorting strap in the front, the antenna would appear capacitive at low frequencies where the cylinder height is small relative to the operating wavelength. The gap and the shorting strap act as an electrically small loop at low frequencies and exhibit inductive behavior. If antenna geometry is optimized by varying the circumference of the gap relative to the cylinder height, the capacitance of the electrically short cylinders can counterbalance the inductance of the electrically small loop formed by the gap, the feed, and the short. In an optimum configuration, the antenna reactance is minimized although the antenna dimensions are small relative to the operating wavelength. Much of our RF Vest research effort for FY 2000 will be directed towards improving the cancellation of the reactances over the widest possible range of frequencies. The goal will be to reduce the low-cutoff frequency to 30 MHz without increasing the overall physical dimensions or the weight of the RF Vest. We are already evaluating different designs with increased gap perimeters, which significantly improves the low-frequency response.

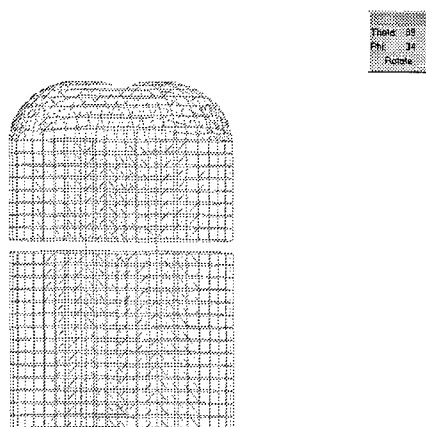


Figure 1. Wire grid model of simple RF Vest antenna. Feed is in back of vest. Shorting is in front.

The RF Vest design cycle involves wire grid model construction using Intellicad/AutoCAD, a model electrical consistency check, and calculations of the antenna parameters such as input impedance and far-field radiation patterns using NEC 4 (GNEC) electromagnetic code. Typically, the simulations are run for the 30- to 500-MHz frequency range in 10-MHz increments. The simulations have been run for the RF Vest in free space, at various heights over a perfect ground, and at 32 inches above an imperfect ground plane with a finite conductivity.

### 3.3 PROTOTYPE CONSTRUCTION

Naval Postgraduate School researchers developed an RF Vest antenna model. Fabricating a prototype was based on this model. Since the time computations on the model were completed, the model was changed to improve the low-frequency response of the RF Vest. Any comparisons between theory and experiment will be made on the original model proposed by the Naval Postgraduate School researchers.



### 3.3.1 Material

The material chosen for the RF Vest antenna was the copper-polyester mixture called FLECTRON, which was developed by the Advanced Performance Materials (APM) Company of St. Louis, Missouri. APM was formerly a division of Monsanto. The material has the advantage of being lightweight, flexible, highly conductive, and breathable. Table 1 lists properties of the material (Advanced Performance Materials Company, 1999).

Table 1. FLECTRON properties (Product No. 3027-106 from APM).

Property	Value	Units
Basis weight	51 to 78	$\text{g/m}^2$
Metal weight	10 to 24	$\text{g/m}^2$
Thickness	0.487	mm
Surface resistivity	<0.1	Ohms/square
Shielding effectiveness	80	dB at 100 MHz
Tensile strength	131/324	N/100 mm
Maximum short-duration temperature	210	$^{\circ}\text{C}$

Approximately 1.5 square meters of the material was used for the RF Vest antenna prototype.

### 3.3.2 Styrofoam Model

To provide consistent mechanical support for the RF Vest antenna with the computer models developed at the Naval Postgraduate School (assumed filled with air), the SSC San Diego Model Shop constructed a Styrofoam model. Styrofoam has electrical properties very similar to air. Figure 2 shows the dimensions of the Styrofoam model compared to a 6 foot tall man. The maximum thickness of the model in the chest area is 8 inches. The corners of the Styrofoam in the chest area have been cut at a 30° angle. The upper part of the model is 20 inches wide. The lower portion of the model is 32 inches high.



Figure 2. Styrofoam model.

### 3.3.3 RF Vest Antenna Fabrication

The RF Vest antenna was fabricated in the SSC San Diego Model Shop. The dimensions were designed so that the RF Vest antenna fit snugly to the Styrofoam model. The lowest part of the RF Vest antenna, the point at which the feed is located, is 32 inches above the ground. Figure 3 shows the front of the RF Vest antenna while it is located on the Styrofoam model. Figure 4 shows the back view. Figure 5 shows the feed for the antenna.



Figure 3. RF Vest antenna (front).



Figure 4. RF Vest antenna (rear).

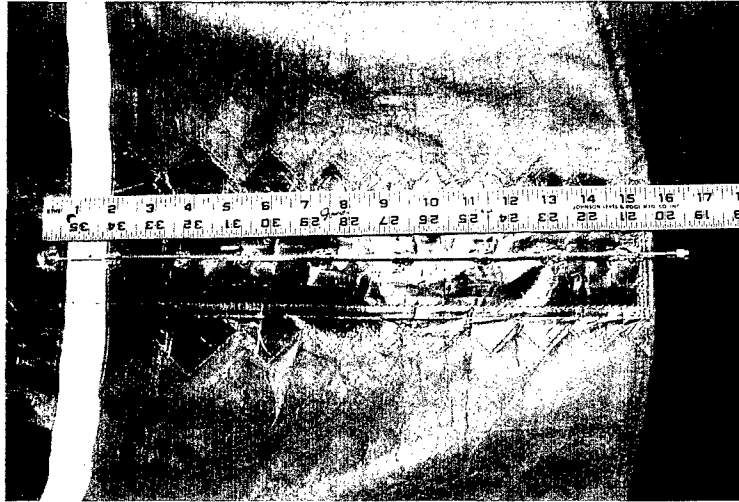


Figure 5. RF Vest antenna feed region.

Copper tape cut in a sawtooth pattern was sewed to the rear bottom half of the RF Vest antenna. A sunburst pattern was sewed to the rear top half the vest. The application of the copper tape permitted easy soldering of the coaxial line shield to the vest. Copper tape was also sewed down the front of the vest. As described in section 3.2, the purpose of the short was to form a loop that increased antenna bandwidth. The sawtooth and sunburst patterns ensured strong electromagnetic coupling between the copper tape and the FLECTRON that makes up the vest.

The FLECTRON material was sewed to a canvas backing cut in the form of a vest. The gap between the vest's upper and lower parts was 1 inch.

In the latter phase of the measurements of the impedance and for all of the pattern measurements, a transformer was inserted into the circuit. The average impedance in the 100- to 500-MHz frequency band was predicted as approximately 120 ohms. The 2:1 transformer (Model T2-1 purchased from Mini-Circuits®) divided this impedance by a factor that varied from 2.5 near 30 MHz to 3.5 near 500 MHz to match efficiently. The insertion was done by cutting the feed at the canvas midpoint and soldering the primary line (pin 6) of the transformer to the feed attached to the lower part of the antenna. The secondary transformer feed (pin 1) was soldered to the sun burst pattern on the upper part of the antenna. The ground of the transformer (pin 3) was soldered to the copper tape on the bottom part of the vest (Mini-Circuits® Catalog, 1997).

### 3.4 PERFORMANCE TEST RESULTS

Although impedance is a more critical measure of performance, the radiation pattern is also important. Impedance is a measure of the transmission efficiency of energy from the transmitter to the antenna. The pattern is the manner in which the antenna radiates energy. Antenna gain is a measure of the efficiency of the far-field radiation. The following subsections discuss measurement results for impedance, radiation pattern, and gain.

### 3.4.1 Impedance

Starting on 31 August 1999, RF Vest antenna impedance measurements were obtained at the SSC San Diego Model Range. The data were obtained from a well-calibrated Hewlett Packard HP 8510C Network Analyzer located under a ground plane. A coaxial line fed through a hole in the ground plane connected the antenna to the network analyzer. Experiments were done with the vest on the Styrofoam model and on a person. When the Styrofoam model was used, the height of the RF Vest antenna above the ground plane could be either 32 or 44 inches. The frequency range was from 30 to 500 MHz. The number of frequencies used in each measurement was 401.

Figure 6 shows the magnitude, real, and imaginary parts of the input impedance as a function of frequency for the RF Vest antenna at 32 inches above the ground plane. Figure 7 shows a comparison of the impedance magnitude for the cases in which the vest is 32 inches and 44 inches above the ground plane. Figure 8 shows a comparison of the VSWR magnitude for the vest on the Styrofoam model and on a person.

The data from figure 6 show the presence of a resonance at a frequency near 100 MHz. The imaginary part of the impedance changes sign from a large positive value to a large negative one. The theoretical model predicted this behavior. The impedance is relatively constant over the frequency range from 150 to 500 MHz. This constancy indicates that with appropriate matching, the RF Vest antenna can radiate efficiently over this fairly large frequency range.

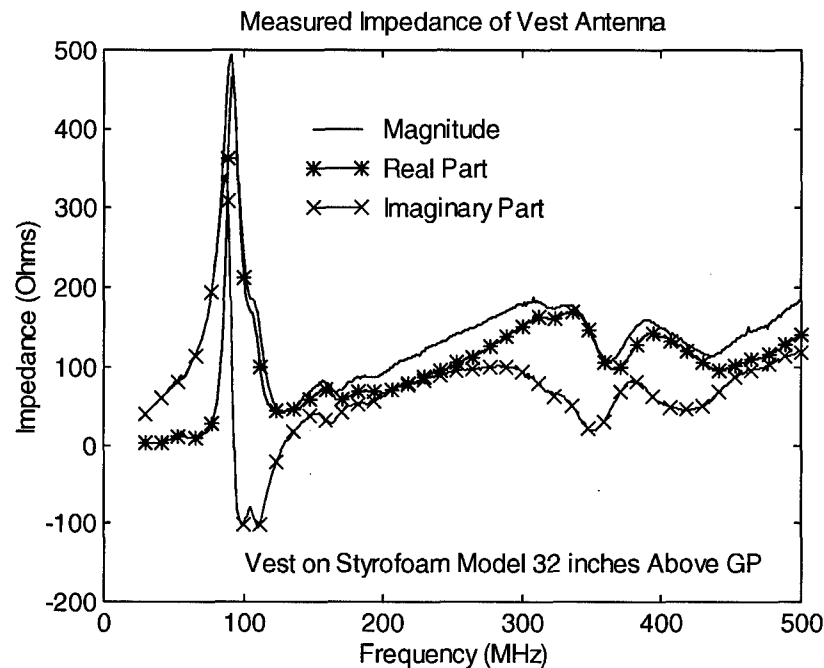


Figure 6. Real, imaginary, and magnitude impedance of RF Vest antenna on Styrofoam model.

Data from figure 7 indicate that the height above the ground plane has little effect upon the magnitude of the impedance. The impedance at the resonance point is somewhat larger if the antenna is higher.

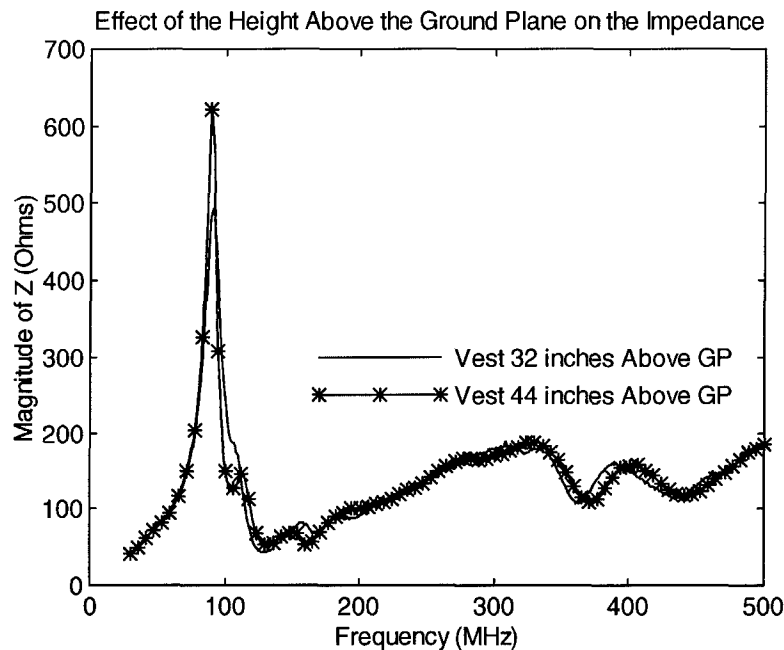


Figure 7. Measured impedance of RF Vest antenna at 32 and 44 inches above ground plane.

Data from figure 8 indicate that the presence of a person has a significant impact upon impedance. This effect is especially prominent at frequencies below 100 MHz. The resonant frequency is lowered. The impedance value at resonance is greatly reduced. Resonance width is also reduced. At frequencies above 150 MHz, the presence of the person tends to smooth the variations in impedance.

Figure 9 shows a comparison of the VSWR of the RF Vest antenna with a transformer in the circuit to one without this device. The transformer reduces the impedance over a wide frequency range by more than 50 percent. Since the predicted and measured impedance is near 125 ohms, the transformer reduces the impedance to a value near that of the coaxial feed (50 ohms). A line has been drawn at the 3:1 line for the VSWR. The data indicate that merely inserting the transformer significantly increases antenna efficiency. Referenced to an impedance of 50 ohms, the vest antenna VSWR is often above 4:1. The VSWR for the vest antenna with the transformer is almost always less than 3:1 for frequencies between 150 MHz and 500 MHz.

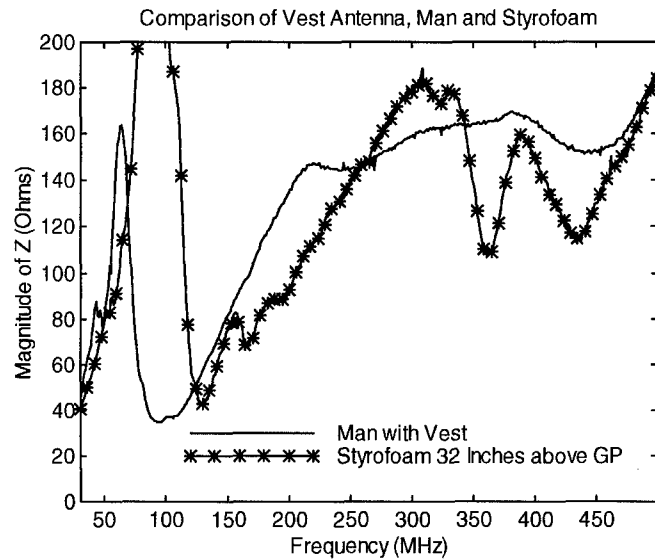


Figure 8. Comparison of measured impedance of RF Vest antenna on Styrofoam model and man.

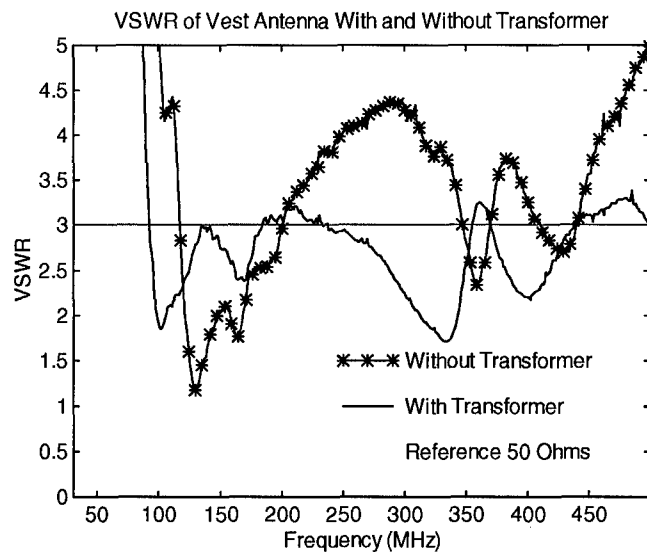


Figure 9. Comparison of measure VSWR of RF Vest antenna with and without transformer.

The development of a matching network reduces the reflection coefficient of the coax-antenna interface. Computer programs developed at SSC San Diego can determine inductance and capacitance values that minimize antenna VSWR.

### 3.4.2 Radiation Patterns

On 20 and 21 September 1999, radiation patterns were measured at the SSC San Diego Pattern Range. The Pattern Range consists of a turntable at the center of a ground plane. The

turntable has a diameter of 16 feet and consists of wood topped by brass plates. The ground plane has a 160-ft diameter and consists of concrete topped by lead. An arch in the form of a tripod is located at the outer rim of the ground plane. The maximum height of the arch is 80 feet.

A common task of the Pattern Range is to measure HF antenna performance on ships. 1/48<sup>th</sup>-scale models weighing hundreds of pounds are placed on the turntable. A log-periodic antenna located on one leg of the arch transmits signals in the 50- to 1500-MHz frequency range. This corresponds to the scaled HF range from 1 to 30 MHz. The transmitter elevation angle can vary between 3 and 90 degrees. The effect of superstructure changes or antenna placement on the performance of HF equipment can be measured at the Pattern Range. These measurements address electromagnetic interference in the HF range.

Figure 10 shows the Pattern Range. Note the turntable at the center of the ground plane, the arch, and various ship models. The azimuth angle,  $\phi = 0^\circ$ , corresponds to the location of the transmitting antenna.

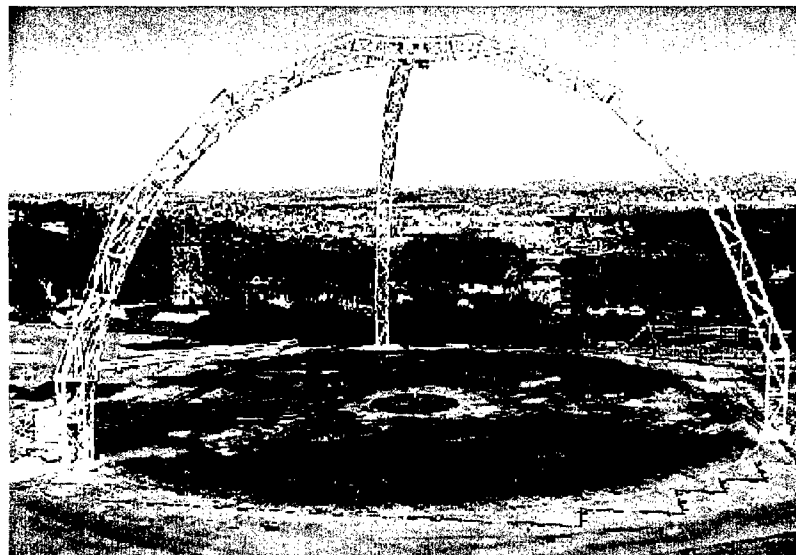


Figure 10. SSC San Diego Pattern Range.

The goal of the experiments was to compare the theoretical predictions with the experimental measurements. Appendix A provides the test plan for the experiments. The elevation angle was changed from  $5^\circ$  to  $85^\circ$  in increments of  $5^\circ$ . The azimuth increment was  $1^\circ$ . The frequency was 100, 200, 300, 400, or 500 MHz. The azimuth angle,  $\phi = 0^\circ$ , corresponds to the front of the vest. With the exception of one set of measurements near the horizon (to determine polarization), the log-periodic antenna was always set in the vertical direction. Except for this case, the measured field was always in the theta direction.

Figure 11 shows the RF Vest antenna on the Styrofoam model at the center of the turntable. The transformer was inserted into the antenna circuit to increase efficiency. Ropes and heavy plates taped to the bottom of the model held the antenna in place. During the afternoon of 20 September, increasing wind speed caused the model to vibrate and possibly turn slightly in azimuth. The experiments of 21 September repeated those of 20 September. Because light rain forced the early termination of the second set of experiments, the maximum elevation angle was  $70^\circ$ . The Pattern Range software automatically changed the measured field so that the output always referred the gain to that of a quarter-wave monopole.



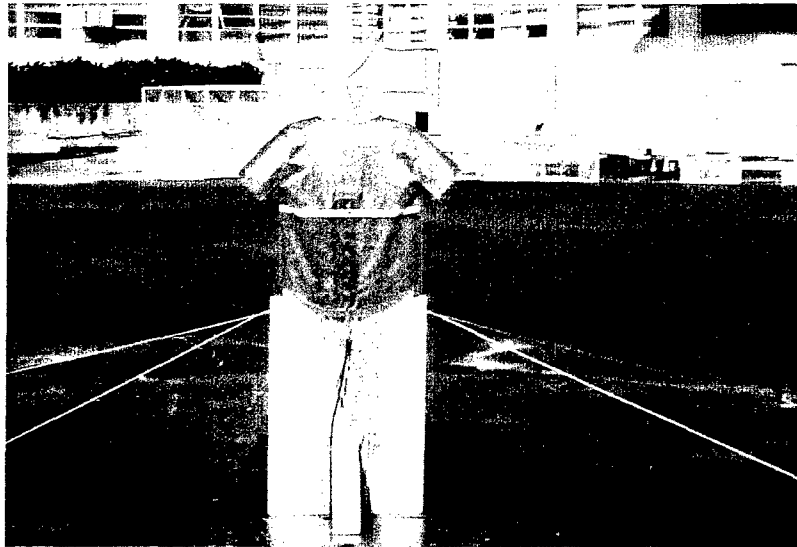


Figure 11. RF Vest antenna and Styrofoam model on Pattern Range.

Figure 12 shows the azimuth pattern of the RF Vest antenna for six elevation angles at a 100-MHz frequency. The gain is a monotonically decreasing function of the elevation angle for all azimuths. Lobes occur with increasing depth as the elevation angle increases. As figure 13 shows, the dependence of the field on elevation angle is no longer monotonic if the frequency is greater than 200 MHz. The dependence is very complicated for these higher frequencies.

Figure 14 shows a comparison of the fields for both vertical and horizontal polarization measured at a  $5^\circ$  elevation angle with 100-MHz frequency. The vertically polarized field is 35 dB higher than the horizontally polarized one for all azimuths. The situation changes as the frequency increases. At  $\phi = 0^\circ$ , the vertically polarized field is always higher than the horizontally polarized one. For other azimuths, the horizontally polarized radiation can be higher than the vertically polarized one. Figure 15 shows the comparison between the measured vertically and horizontally polarized fields versus azimuth for the higher frequencies.

Figure 16 shows the field at  $\phi = 0^\circ$  as a function of elevation angle for five frequencies. For all frequencies, there is at least one lobe at an intermediate elevation angle (besides the expected one at a  $90^\circ$  elevation angle). Figures 16 and 17 show the measured field at  $\phi = 0^\circ$  versus elevation angle at the frequencies 100 and 500 MHz, respectively. As expected, the number of lobes increases as the frequency increases. Corresponding data for  $\phi = 90, 180$ , and  $270^\circ$  show similar behavior. The measured data are highly symmetrical in the  $\phi = 90^\circ$  and  $\phi = 270^\circ$  directions. The measured data are similar in the  $\phi = 0^\circ$  and  $180^\circ$  directions for all but the highest frequencies.

The measurement data on the 2 days are very similar. At the frequencies of 100, 200, and 300 MHz, the maximum deviation is 1.64 dB at a  $5^\circ$  elevation angle. This deviation increased to 3.1 and 5.4 dB at frequencies of 400 and 500 MHz, respectively. As the elevation angle increased to  $50^\circ$ , the deviation increased with increasing frequency. The null location pattern, however, did not change. Also the value of the maximum field did not differ by more than 2 dB. The value of the fields at the nulls was the primary difference in the data of the 2 days.

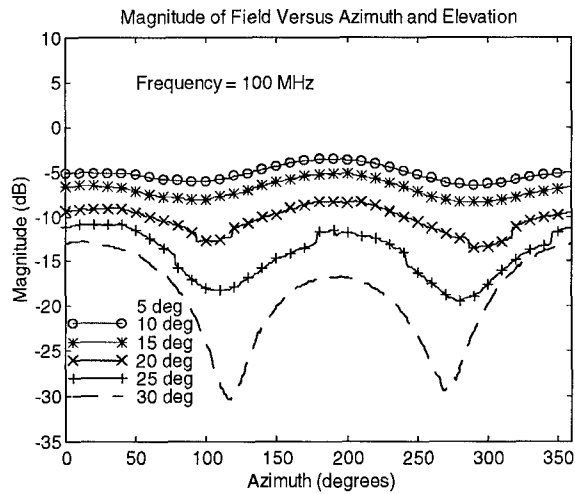


Figure 12. Experimentally determined fields from RF Vest antenna versus azimuth for six elevation angles and 100-MHz frequency.

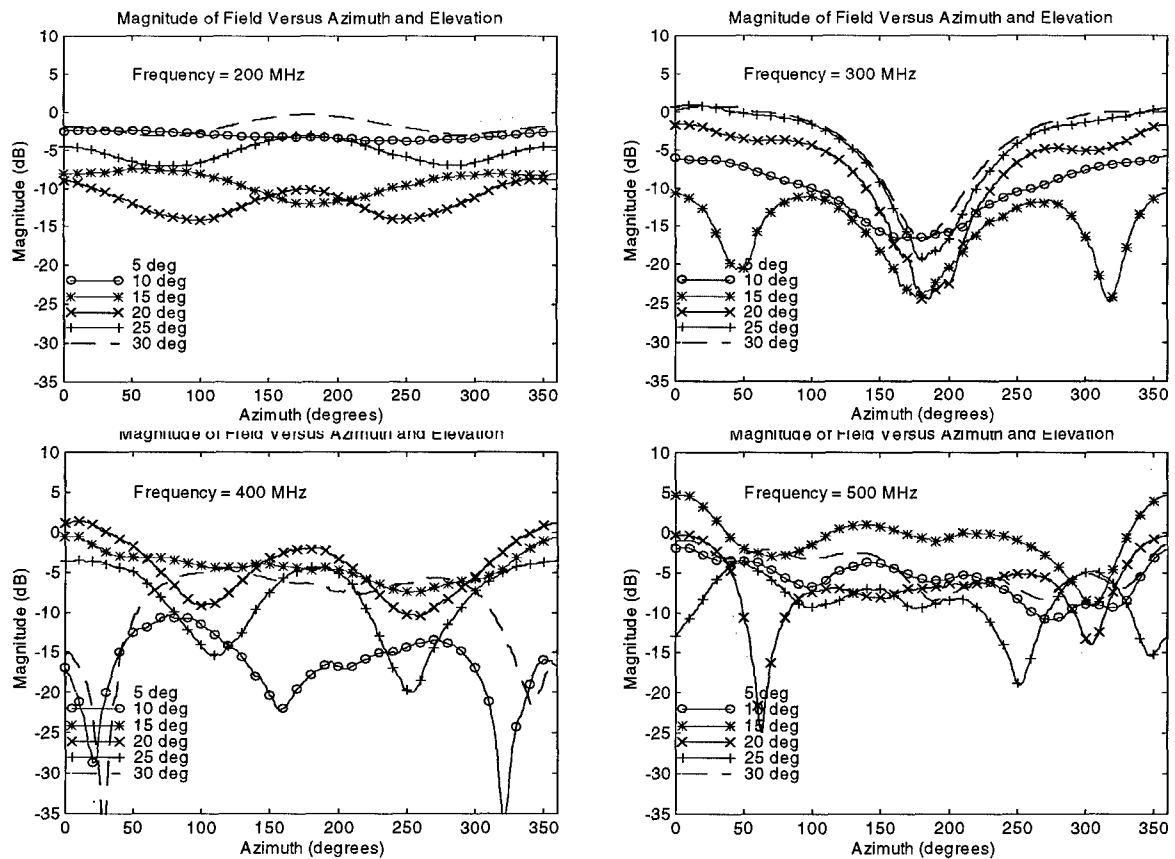


Figure 13. Experimentally determined fields from RF Vest antenna versus azimuth for six elevation angles and frequencies of 200, 300, 400, 500 MHz.

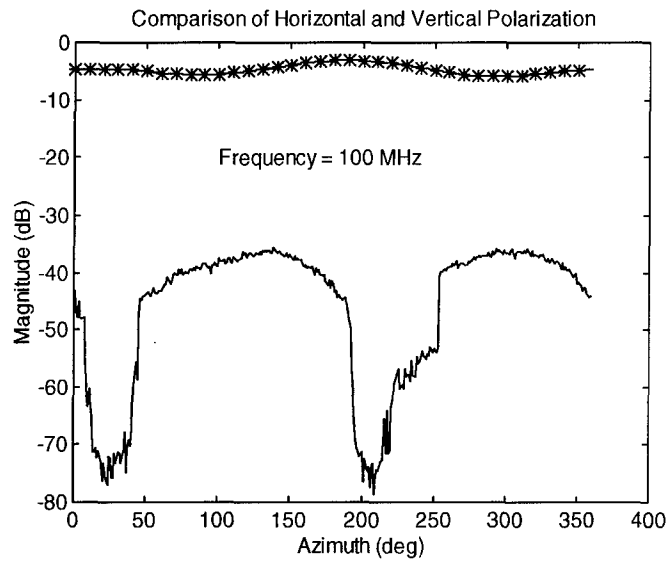


Figure 14. Experimentally determined field with horizontal and vertical polarization versus azimuth at a 100-MHz frequency. The elevation angle is  $5^\circ$ . In figures 14 and 15, the fields with horizontal polarization are solid lines. Those with vertical polarization have asterisks superposed on the lines.

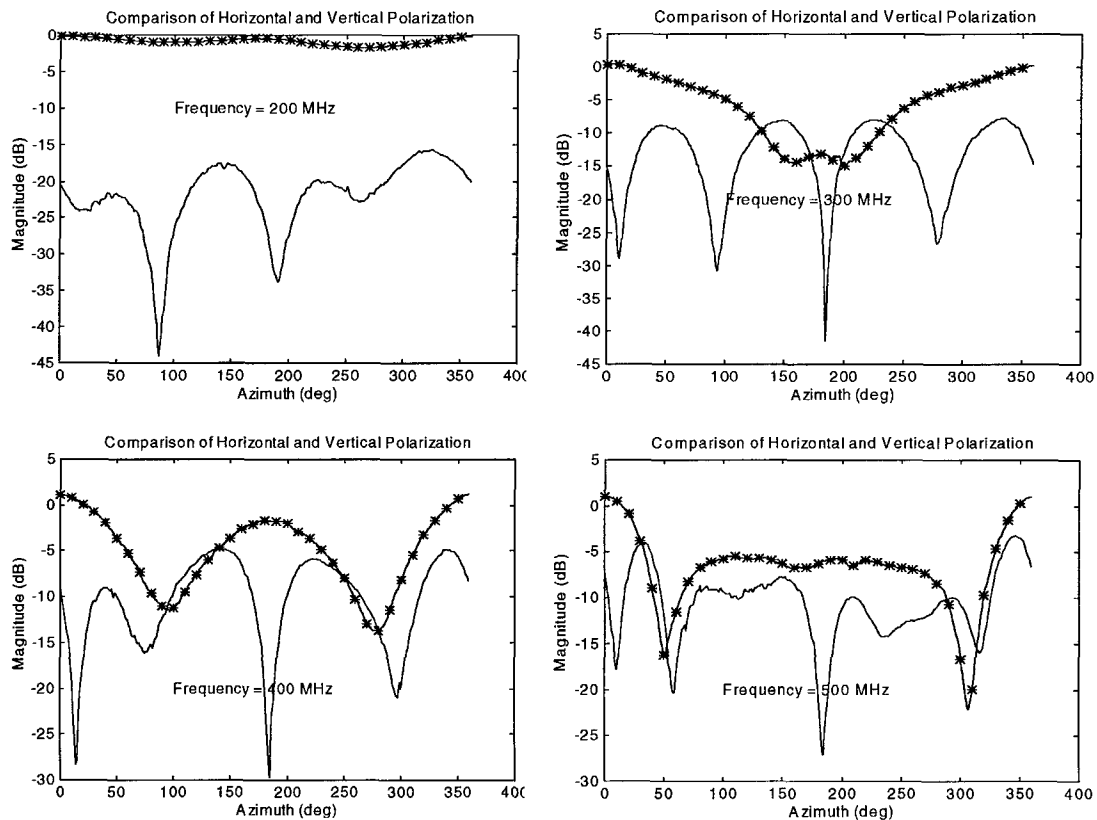


Figure 15. Experimentally determined fields with horizontal and vertical polarization versus azimuth for 200-, 300-, 400-, and 500-MHz frequencies. Elevation angle is  $5^\circ$ .

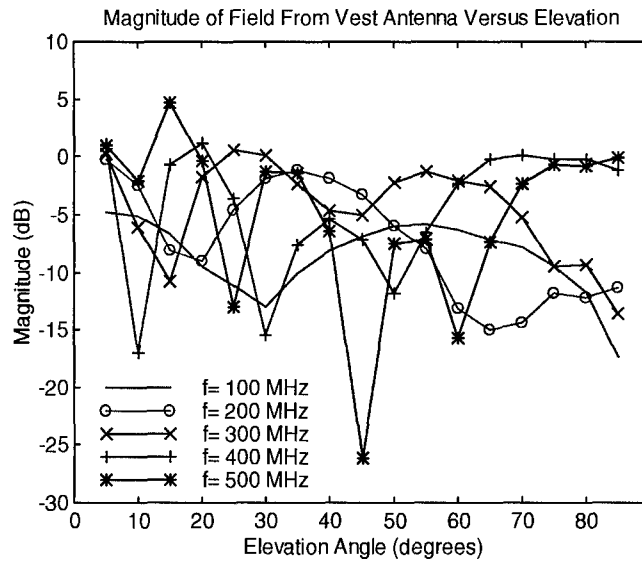


Figure 16. Experimentally determined fields versus elevation angle for 100-, 200-, 300-, 400-, and 500-MHz frequencies. The azimuth angle is  $0^\circ$ .

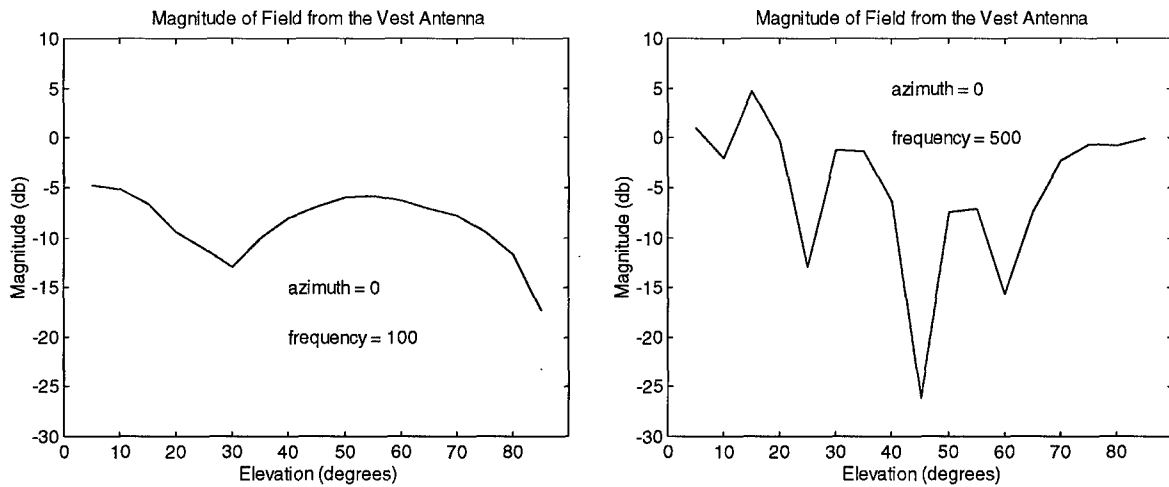


Figure 17. Experimentally determined field versus elevation angle at 100- and 500-MHz frequency.

## 4. THEORY AND EXPERIMENT RESULT/COMPARISON/ANALYSIS

The previous sections described the models and tools used for computing the fields from the vest antenna. The most important aspect of the FY 1999 effort was to confirm the validity of the predictions. The areas in which comparisons can be made are impedance, azimuth radiation patterns, and elevation radiation patterns. The following subsections discuss each area.

### 4.1 IMPEDANCE

As figure 7 shows, the vest impedance that is 32 inches above the ground plane is almost the same as that for a 44-inch height. Figure 18 shows the comparison between theory and experiment for the vest impedance magnitude as a frequency function. Comparisons for the real and imaginary part have a similar character. The ratio of theoretical to experimental impedance corresponding to the resonant point (near 100 MHz) is approximately 2. Theory predicts a much higher impedance because of its use of an ideal conductor. The real antenna has a large but finite conductivity.

Figure 19 shows the ratio of the theoretical to experimentally determined impedance. Figure 20 presents the results for a vest that is 44 inches above the ground plane with a change in vertical scale to emphasize the frequency regime in which the vest works best as an antenna. The primary discrepancy between theory and experiment occurs at a frequency of approximately 350 MHz. The antenna modeling tools used so far do not have the ability to model the coax feed. At a frequency near 350 MHz, the wavelength is 33.8 inches. The half-wavelength is only slightly less than the length of the feed region. There is probably a feed section resonance not modeled by the theory that causes the discrepancy. For most of the frequency band between 150 and 500 MHz, the agreement between theory and experiment is within 10 percent. Even at its worst, the magnitude of the impedance is within a factor of 2.2 for all frequencies between 30 and 500 MHz.

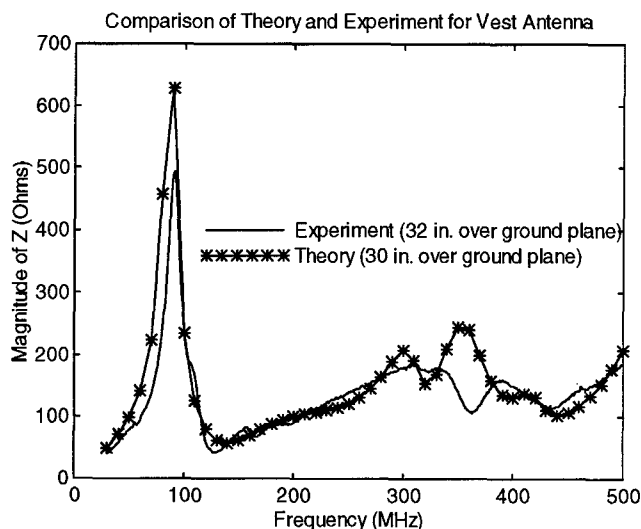


Figure 18. Comparison of experimentally and theoretically determined impedance magnitude versus frequency. Antenna height above ground plane is 32 inches.

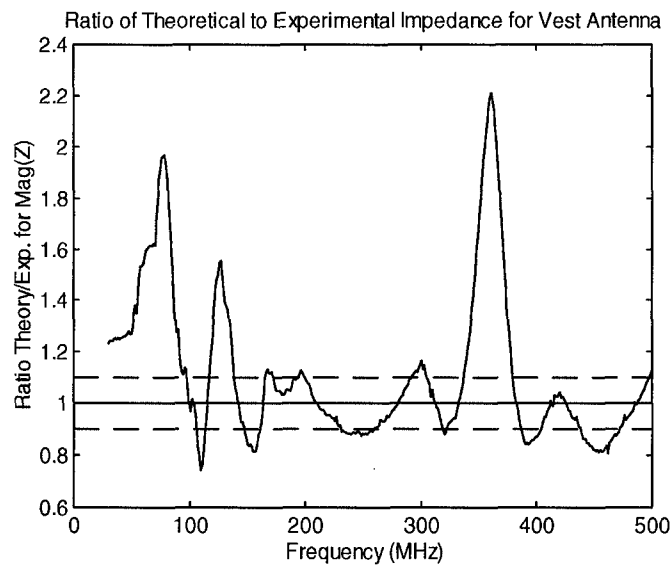


Figure 19. Ratio of theoretically determined absolute impedance magnitude to that experimentally determined versus frequency of RF Vest antenna.

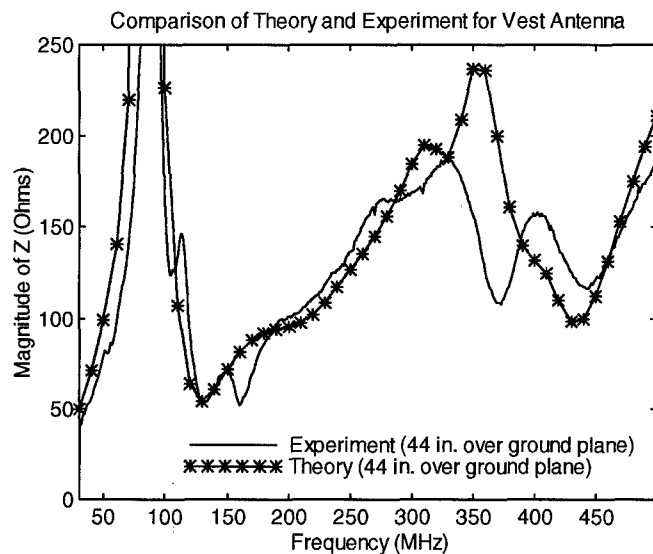


Figure 20. Comparison of theory to experiment for the absolute impedance magnitude. RF Vest antenna height above ground plane is 44 inches.

Impedance is one of the most sensitive measures of antenna performance. Agreement between theory and experiment is within 10 percent without any adjustable parameters.

#### 4.2 RADIATION PATTERNS IN AZIMUTH

Figure 21 shows a comparison between theory and experiment for the 100-MHz azimuth pattern. Both theory and experiment indicate that the pattern is largely isotropic. For this and the other four azimuth patterns to be presented, there is one adjustable parameter. This is the overall level of the pattern. The theory predicts the directivity as a function of angle and frequency. The gain is the measured quantity that includes the reflection effects caused by mismatch and losses within the antenna itself. The theory was normalized so that the experimental and theoretical fields were equal at  $\phi = 0^\circ$ . Figures 22, 23, 24, and 25 present the corresponding comparisons at 200, 300, 400, and 500 MHz.

The agreement between theory and experiment is fairly good. For most of the patterns, the nulls and maximums occur at the same azimuth.

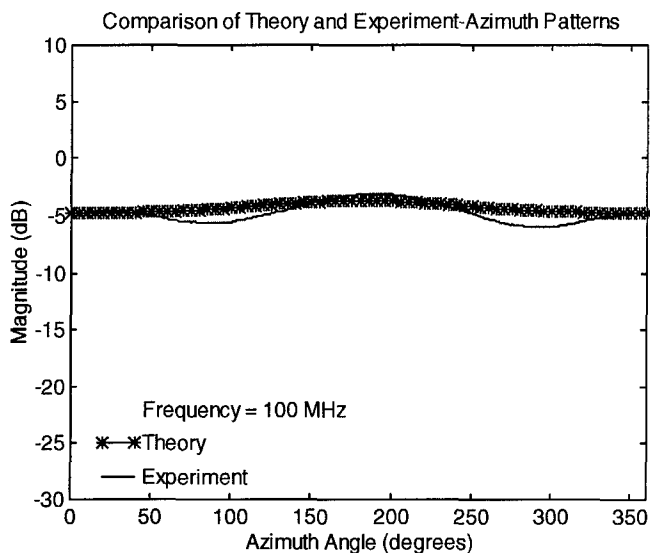


Figure 21. Comparison between experimentally determined fields at  $5^\circ$  elevation angle and theoretical predictions for 100-MHz frequency.

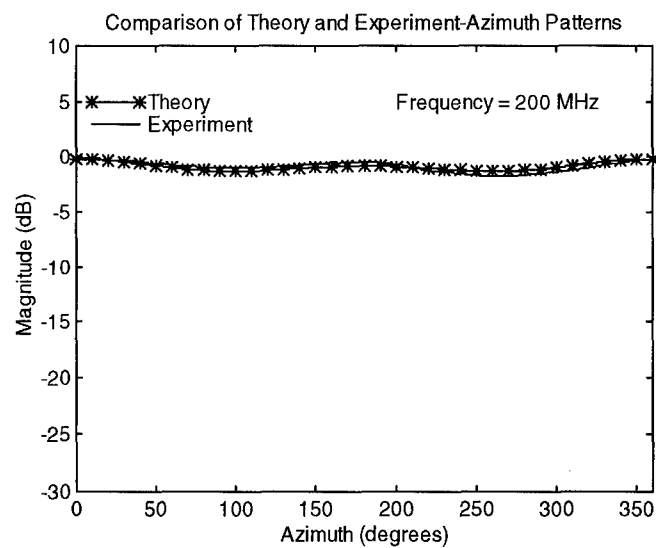


Figure 22. Comparison between experimentally determined fields at 5° elevation angle and theoretical predictions for 200-MHz frequency.

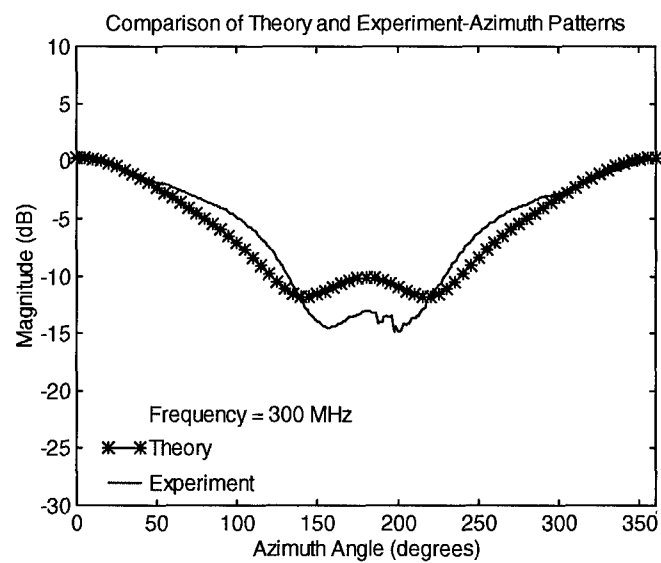


Figure 23. Comparison between experimentally determined fields at 5° elevation angle and theoretical predictions for 300-MHz frequency.



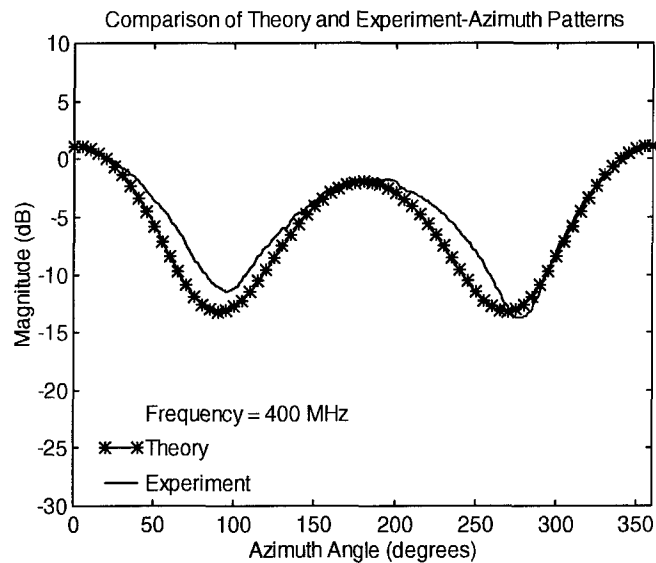


Figure 24. Comparison between experimentally determined fields at 5° elevation angle and theoretical predictions for 400-MHz frequency.

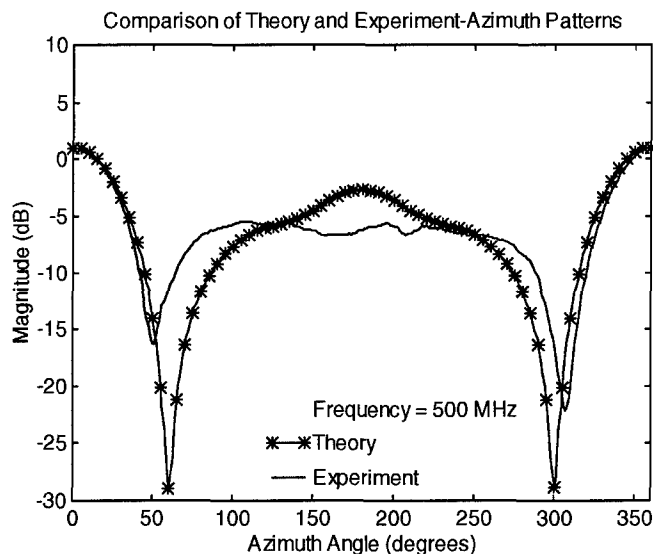


Figure 25. Comparison between experimentally determined fields at 5° elevation angle and theoretical predictions for 500-MHz frequency.

#### 4.3 RADIATION PATTERNS IN ELEVATION

The theoretical elevation pattern shows significant dependence on the assumed value of the ground plane conductivity. The assumption of a perfectly conducting ground plane causes the predicted results to have a marginal correlation with the observation. The assumption of a finite conductivity (assumed as lead, 4.6 MS/m) leads to the following results.

The theta component of the electric field was measured during the experiment on the Pattern Range. The absolute levels in the plots below were adjusted so that the maximum of

both theory and experiment was equal to 0 dB. The value plotted in the graphs below is 20 times the logarithm of the theoretically predicted absolute value of the theta component of the electric field. Figure 26 presents the comparison between theory and experiment for the field versus elevation angle for a 100-MHz frequency. Figures 27, 28, 29, and 30 present the corresponding comparisons between theory and experiment for the elevation patterns for 200, 300, 400, and 500 MHz, respectively.

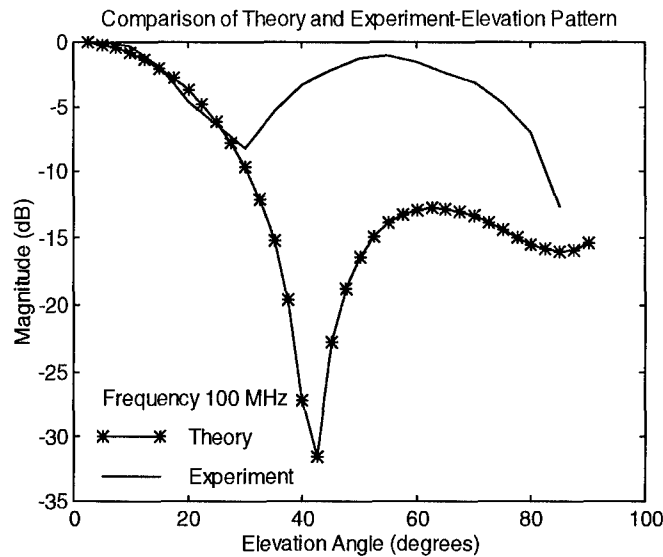


Figure 26. Comparison between experimentally determined fields versus elevation angle and theoretical predictions for 100-MHz frequency and  $\phi = 0^\circ$ .

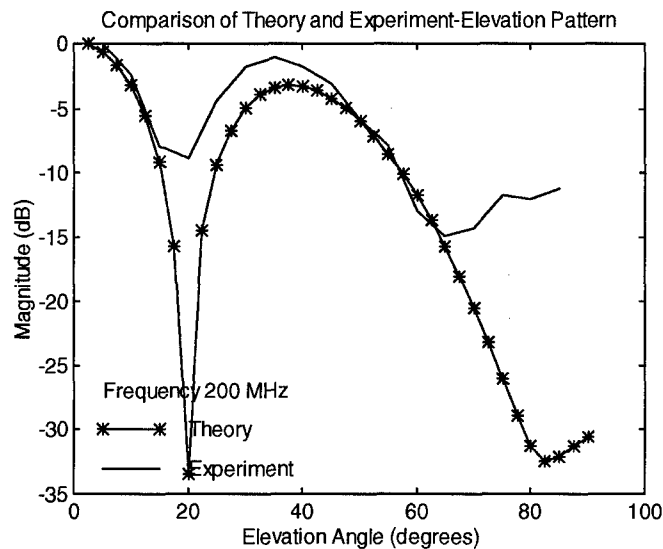


Figure 27. Comparison between experimentally determined fields versus elevation angle and theoretical predictions for 200-MHz frequency and  $\phi = 0^\circ$ .

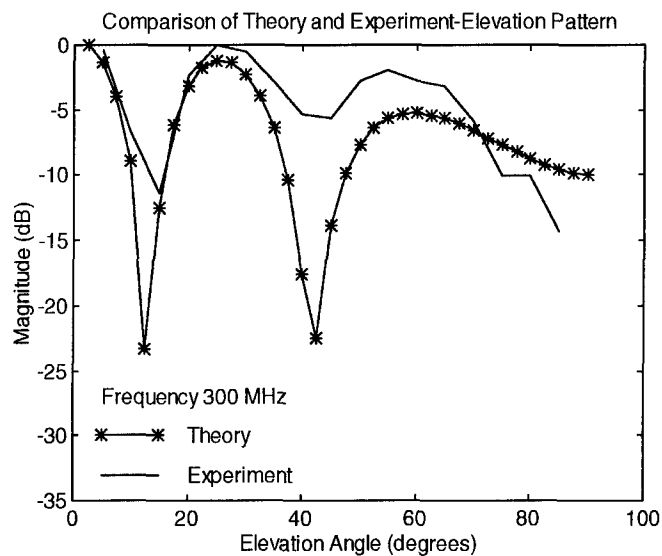


Figure 28. Comparison between experimentally determined fields versus elevation angle and theoretical predictions for 300-MHz frequency and  $\phi = 0^\circ$ .

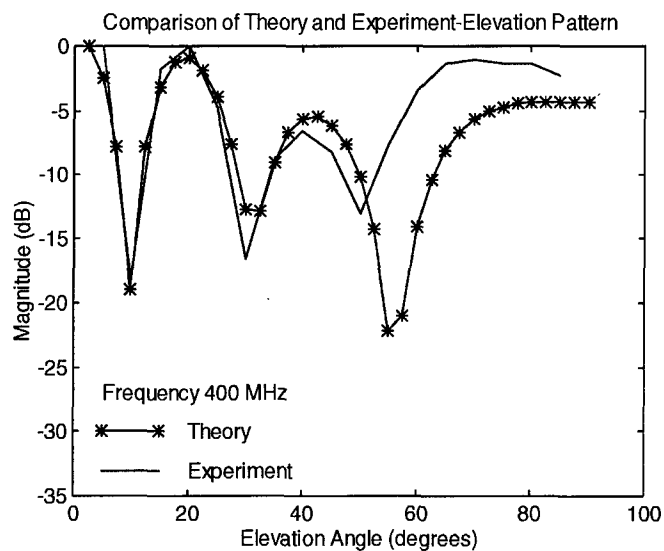


Figure 29. Comparison between experimentally determined fields versus elevation angle and theoretical predictions for 400-MHz frequency and  $\phi = 0^\circ$ .

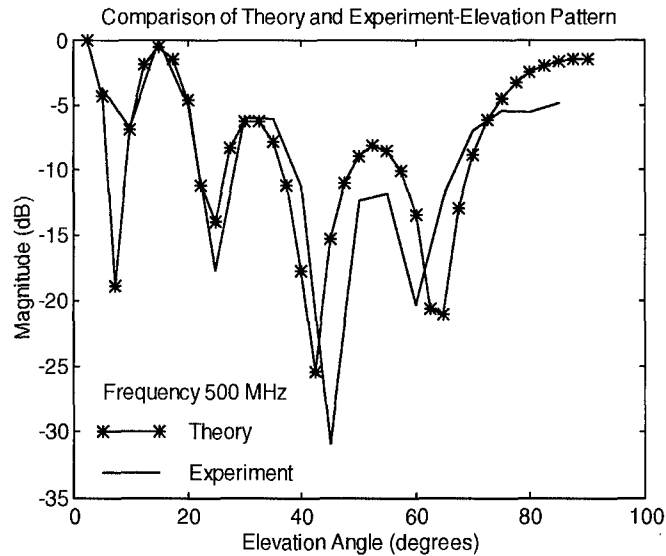


Figure 30. Comparison between experimentally determined fields versus elevation angle and theoretical predictions for 500-MHz frequency and  $\phi = 0^\circ$ .

The major discrepancy is at the lowest frequency of observation, 100 MHz. For the other frequencies, there is good correlation between theory and experiment. The predicted locations of the nulls are very close to those observed. The predicted null depth is usually much larger than those observed. This disparity of null depth was also observed in the azimuth patterns. Real materials with complex impedance tend to decrease the height of peaks and the depth of nulls. The agreement between theory and experiment increases as the frequency increases.

Note that the pattern range has a discontinuity in the conductivity at the turntable/ground plane junction. This discontinuity should affect some of the measurements at the highest elevation angles.

## 5. CONCLUSIONS

The purpose of the FY 1999 effort was to develop the preliminary design of a candidate man-carried antenna, predict performance, and fabricate a prototype. The prototype provides a means to test the validity of the predictions. The testing would involve measuring the impedance and radiation patterns in both azimuth and elevation direction. These goals were accomplished.

A comparison between theoretical and experimental determination of the impedance demonstrates that the Naval Postgraduate School model is good for most frequencies. The resonance (near 100 MHz) is well-modeled. The greatest discrepancy is near the resonant feed frequency. The tools used do not model feed region details. The discrepancy, confined to a small band of frequencies, is not excessive. Although a more sophisticated treatment of the feed region would probably resolve this issue, such a task has little merit since the measured impedance results show that the antenna is more efficient than predicted. Efforts should focus on improving the efficiency of RF Vest antenna design and bandwidth rather than changing the model to fit measured data.

The azimuth patterns are well-represented by the theoretical models. The locations of the nulls and maximums as well as their relative values are accurately predicted. Similarly, the elevation patterns at frequencies larger than 100 MHz are also well-represented by the theoretical models.

The presence of the person in the RF Vest antenna has a significant effect upon impedance. At the lowest frequencies (less than 100 MHz), the presence of the person reduces the resonance. The overall effect is to improve the antenna bandwidth by extending the operating range to lower frequencies.

The RF Vest antenna operates most efficiently at frequencies in which the electrical length is commensurate with the operating wavelength. At frequencies for which the antenna dimensions become large compared to the operating wavelength, nulls and maximums occur at several angles in both azimuth and elevation.

Even a simple device such as a transformer should increase antenna efficiency of the antenna by matching the impedance to that of the coax. More sophisticated techniques such as the development of a matching circuit would optimize the efficiency to acceptable values.

The material used in making the RF Vest antenna is excellent. The qualities of light weight, high conductivity, high flexibility, and breathability recommend this copper and polyester material.

## **6. RECOMMENDATIONS**

### **6.1 RF VEST ANTENNA OPTIMIZATION**

Research should continue on the RF Vest antenna. The vest should serve as the primary JTR antenna since its likely frequency band will encompass many of the most important ones for LOS communications. Non-metallic substances such as dielectric cladding should be avoided. These add weight and reduce overall antenna efficiency. Patterns cut into the RF Vest antenna should be investigated to increase antenna bandwidth, especially to reduce the low cutoff frequency. The approach and tools validated in the FY 1999 effort should be used for the FY 2000 optimization design phase. A new prototype should be constructed for an optimized design capable of the full 30- to 500-MHz frequency range. The FY 1999 vest antenna already covers the 150- to 500-MHz range. Most of the effort in FY 2000 should be directed to reducing the lowest operational frequency to 30 MHz.

RF Vest antenna polarization does not remain purely vertical for all azimuth angles, especially at higher frequencies. This should be researched very thoroughly because of the polarization requirement of most legacy equipment.

### **6.2 HELMET ANTENNA DEVELOPMENT**

Fractal-like geometry offers a novel approach to attaining the 500- to 2000-MHz frequency band. The theoretical model will be a physically small antenna fitted atop a standard-issue Kevlar helmet. New software tools will be needed to model the interaction of the elements with the Kevlar material. After developing a theoretical model that shows promise of efficiency in the 500- to 2000-MHz band, a prototype should be fabricated. The actual model will demonstrate the validity of the computer model, provide for guideposts for future research, and determine the effects of the interaction between the person and the antenna. (The interaction between the experiment and the theory is usually beneficial to both.) The helmet antenna should be designed such that the low end of its operating frequency overlaps with the high end of RF Vest antenna operating frequency. The overlap will prevent a gap in JTR frequency coverage.

### **6.3 ASSESSMENT OF INTERACTION BETWEEN PERSON AND ANTENNA**

The proximity between the RF Vest antenna and the wearer-operator requires significant research in their mutual interaction. As shown by the experimental results of the RF Vest antenna, the person affects the impedance and its performance, especially at frequencies less than 100 MHz. Correspondingly, the antenna affects the person. The degree of irradiation of the person and the hazards engendered must be documented and mitigated. Steps must be taken in the vest and helmet antenna design to maintain RF energy absorption levels that are acceptable based upon applicable standards. A well-coordinated program should be set up to predict antenna near-field strength, measure the fields and compare them to predictions, and reduce exposure. The RF Vest antenna, because it surrounds the person, is actually more likely to shield its wearer than a whip design.

#### **6.4 HF ANTENNA**

Research should proceed on the HF antenna. This subsystem probably has the furthest to go before fielding a prototype. The engineering demands of a small-size HF device are very high. A tuning device will probably be needed for the HF antenna.

#### **6.5 FULL SYSTEM**

Research must be done, probably in FY 2001, to treat the three antennas as a system. Interactions between the subsystems must be considered. Electromagnetic interference must be considered and mitigated to field a useful system in the appropriate frequency range. Methods for signal hand-off for one antenna to those in another must be researched and applied.

## 7. REFERENCES

- Advanced Performance Materials Company. 1999. Data sheet for FLECTRON. St. Louis, MO.
- Dilworth, I. J. 1994. "Low Profile Wideband Antenna for DECT Applications," *IEE Colloquium on Radio Frequency Design in Mobile Radio Transceiver*, p. 7/1–7/3.
- Fujimoto, K. and J. R. James. 1994. *Mobile Antenna Systems Handbook*. Artech House, Norwood, MA.
- Fujimoto, K., A. Henderson, K. Hirasawa, and J. R. James. 1997. *Small Antennas*. John Wiley & Sons, New York, NY.
- Mini-Circuits® Catalog. 1997. Brooklyn, NY, pp. 14–16.
- Puente-Baliarda, C. and R. Pous. 1996. "Fractal Design of Multiband and Low Side-Lobe Arrays," *IEEE Transactions on Antennas and Propagation* (May), p. 730–739.
- Rumsey, V. H. 1966. *Frequency Independent Antennas*. Academic Press, New York, NY.
- Strugatsky, A. and C. H. Walter. 1992. "Multimode Multiband Antenna," *Proceedings of the Tactical Communications Conference*, vol. 1, p. 281–295.
- Tripp, V. K. 1995. "The Spiral-Mode Microstrip Antenna—Broad Bandwidth and Low Profile," *IEEE International Symposium on Electromagnetic Compatibility, Symposium Record*, p. 108–113.
- Werner, D. H. and P. L. Werner. 1996. "Frequency-Independent Features of Self-Similar Antennas," *Radio Science* (Nov–Dec), p. 1331–1343.

Note: This is a list of the most relevant references used for this report and is not an exhaustive list covered in the survey.



## **APPENDIX A**

### **TEST PLAN FOR IMPEDANCE AND RADIATION PATTERN MEASUREMENT OF THE RF VEST**

#### **GOALS**

There are two goals for the experiments on the man-carried, broadband antennas to be conducted during August and September 1999. The first is to measure such parameters as the impedance and return loss. Such measurements characterize the flow of energy from the circuit to the antenna. The second is to measure the pattern. The radiation pattern is a measure of the manner in which energy flows from the antenna to an observer.

#### **BACKGROUND**

Researchers at the Naval Postgraduate School have designed an all metal version of a wearable antenna. They have made predictions on the impedance, VSWR, and pattern as a function of frequency. The design has been given to the SPAWAR Systems Center in San Diego. A vest antenna (Mark I) has been fabricated by the SSC San Diego Model Shop. The material for construction of the antenna is a metallized cloth developed by APM in St. Louis. The Model Shop has also fabricated a dummy made of Styrofoam that is close to the size of a large person.

In mid-October, the Model Shop will make a second vest (Mark II). The difference between the two models is the pattern in the metal fabric. Theoretical predictions indicate that with a particular pattern, the VSWR will be 3:1 or less for the 30- to 100-MHz and 200- to 500-MHz frequency ranges.

#### **IMPEDANCE MEASUREMENTS**

Originally, the plan was to use the Hewlett-Packard HP 8510C Network Analyzer. Recently, SSC San Diego obtained the "Site Master." This device weighs approximately 4 pounds. Its measurements correspond precisely to those of the 8510C. The output is the magnitude and phase of the reflection coefficient from the antenna. Using standard formulas, these data can be converted to the real and imaginary parts of the impedance. The frequency bounds of the device are 5 MHz to 1200 MHz.

Such a portable device provides several opportunities that the less-portable 8510C would make very difficult. Four different measurements will be obtained. There will be the Styrofoam and a real person. There will be measurements obtained over a ground plane and over dirt. Possibly several different sites will be used to make the measurements to provide a measure of the sensitivity of the impedance to the type of dirt.

The data will be output to a floppy disk and input to MATLAB programs. The data will be sent as an e-mail attachment to the Naval Postgraduate School as soon as practical.

#### **PATTERN MEASUREMENTS**

The pattern measurements should be obtained at the Pattern Range. The transmitting antenna will be a log-periodic with well-calibrated gain. During the month of September, the

receiving antenna will be the first antenna. During the month of December, the second vest will be tested. The Model Range has a signal generator for use in the proper frequency range (100 to 500 MHz). One version of the transmitting antenna is well-calibrated within a frequency range between 96 MHz and 1500 MHz. The transmitting antenna will be located on the arch. The receive antenna will be located on the turntable. A Styrofoam dummy will be used to keep the vest antenna in its proper location and orientation.

The pattern measurements will be of two types. The first will be the measurement of the pattern at one elevation ( $\theta = 85^\circ$ ) in the azimuth direction. Measurements should be taken at the frequencies at which predictions have been made. That is, the frequencies should be 100, 200, 300, 400, and 500 MHz. The orientation of the transmitting antenna should be changed from vertical to horizontal to determine the polarization as a function of azimuth and frequency at the horizon. All other measurements should be done only with vertical polarization. The second type is an elevation pattern at  $\phi = 0^\circ$ . One limitation of the Pattern Range is that there is no provision for an elevation cut. The transmitting antenna can be positioned at various elevation angles while the azimuth changes. The predictions indicate that there should be at least one null in the range of elevation angles  $5^\circ$  to  $85^\circ$  for all frequencies. An interval of  $5^\circ$  should bracket the position of this null. The most important measurement is to obtain the complete volumetric pattern for each type of vest.

The data will be digitized and translated into ASCII format for later comparison with the predictions. The data will be transferred to floppy disk. Copies will be sent to the Naval Postgraduate School.

The absolute gain as a function of frequency and angle should be measured. The Pattern Range is extremely well calibrated. Experience has shown that the calibration remains the same over a duration of weeks. The calibration phase can thus be shortened. A vertical monopole is the calibration antenna used for obtaining values of the gain.

We should assume approximately a day to set up. The Pattern Range is used constantly. The equipment is well maintained. Table A-1 describes the minimum set of measurements to be obtained. A total of 2 weeks have been set aside for the pattern measurements during the months of September and December.

If everything is working perfectly, each azimuth measurement requires 30 seconds. A change in frequency and formatting of the data require an additional 30 seconds. Allowing for additional delays, 3 minutes are required to perform each azimuth run. The Pattern Range is well automated. When the elevation angle is changed, an additional 5 minutes are required. No changes in transmitting antenna are required. The big log-periodic can handle all frequencies from 100 to 1500 MHz.

Table A-1. Program of measurements for the two vests.

Calibration	Quarter Wave Monopole	V
Frequency (MHz)	Elevation Angle (degrees)	Polarization
100	5	V
200	5	V
300	5	V
400	5	V
500	5	V
Azimuth Measurements		
100	5	V
200	5	V
300	5	V
400	5	V
500	5	V
100	5	H
200	5	H
300	5	H
400	5	H
500	5	H
100	10	V
200	10	V
300	10	V
400	10	V
500	10	V

Table A-1. Program of measurements for the two vests. (continued)

Calibration	Quarter Wave Monopole	V
Frequency (MHz)	Elevation Angle (degrees)	Polarization
100	15	V
200	15	V
300	15	V
400	15	V
500	15	V
100	20	V
200	20	V
300	20	V
400	20	V
500	20	V
100	25	V
200	25	V
300	25	V
400	25	V
500	25	V
100	30	V
200	30	V
300	30	V
400	30	V
500	30	V
100	35	V
200	35	V

Table A-1. Program of measurements for the two vests. (continued)

Calibration	Quarter Wave Monopole	V
Frequency (MHz)	Elevation Angle (degrees)	Polarization
300	35	V
400	35	V
500	35	V
100	40	V
200	40	V
300	40	V
400	40	V
500	40	V
100	45	V
200	45	V
300	45	V
400	45	V
500	45	V
100	50	V
200	50	V
300	50	V
400	50	V
500	50	V
100	55	V
200	55	V
300	55	V
400	55	V

Table A-1. Program of measurements for the two vests. (continued)

Calibration	Quarter Wave Monopole	V
Frequency (MHz)	Elevation Angle (degrees)	Polarization
500	55	V
100	60	V
200	60	V
300	60	V
400	60	V
500	60	V
100	65	V
200	65	V
300	65	V
400	65	V
500	65	V
100	70*	V
200	70*	V
300	70*	V
400	70*	V
500	70*	V
100	75*	V
200	75*	V
300	75*	V
400	75*	V
500	75*	V
100	80*	V

Table A-1. Program of measurements for the two vests. (continued)

Calibration	Quarter Wave Monopole	V
Frequency (MHz)	Elevation Angle (degrees)	Polarization
200	80*	V
300	80*	V
400	80*	V
500	80*	V
100	85*	V
200	85*	V
300	85*	V
400	85*	V
500	85*	V

\* If the patterns at lower elevation angles indicate that the level is more than 10 dB below the peak at the horizon, these might not be done.

## ANALYSIS

After each day's experiment there should be a quick-look analysis to ensure the data have no dropouts. The ASCII files should be previewed to ensure the data are readable.

MATLAB should be used for analyzing the data. The data should be compared with the predictions for both patterns and impedance.

One graph should be the predicted magnitude of the impedance of the two types of antennas versus frequency (from 100 to 500 MHz). Overlaying this graph should be the experimental data.

There will be the writing of a report describing the goals, set up, and results of the experiment. This should be complementary to the report that researchers at the Naval Postgraduate School will write on the calculations and design of the vests. The report will have graphs such as those described above. Other graphs should be the absolute gain (determined by comparing the test measurement with the calibration measurement in the standard manner) as a function of azimuth. Overlaying this graph should be the predicted values from the predictions. The elevation pattern will be obtained by extracting the one measurement from every azimuth run that pertains to  $\phi = 0^\circ$ . There should be one graph for every type of azimuth and elevation pattern measured. The report will describe the comparison between theory and experiment.

**REPORT DOCUMENTATION PAGE**Form Approved  
OMB No. 0704-0188

Public reporting burden for this collection of information is estimated to average 1 hour per response, including the time for reviewing instructions, searching existing data sources, gathering and maintaining the data needed, and completing and reviewing the collection of information. Send comments regarding this burden estimate or any other aspect of this collection of information, including suggestions for reducing this burden, to Washington Headquarters Services, Directorate for Information Operations and Reports, 1215 Jefferson Davis Highway, Suite 1204, Arlington, VA 22202-4302, and to the Office of Management and Budget, Paperwork Reduction Project (0704-0188), Washington, DC 20503.

1. AGENCY USE ONLY (Leave blank)		2. REPORT DATE  June 1999	3. REPORT TYPE AND DATES COVERED  Final
4. TITLE AND SUBTITLE  FISCAL YEAR 1999 WIDEBAND ANTENNA FEASIBILITY STUDY Man-Carried Ultrawideband Antenna System		5. FUNDING NUMBERS  PE: 0602131M AN: DN304029 WU: CAB1	
6. AUTHOR(S) R. C. Adams LCDR C. P. Haglind LCDR (sel.) H. N. Pace, Jr. SSC San Diego J. Lebaric R. Adler CAPT T. M. Gainor A. T. Tan Naval Postgraduate School			
7. PERFORMING ORGANIZATION NAME(S) AND ADDRESS(ES)  SSC San Diego San Diego, CA 92152-5001		8. PERFORMING ORGANIZATION REPORT NUMBER  TR 1808	
9. SPONSORING/MONITORING AGENCY NAME(S) AND ADDRESS(ES)  Amphibious Warfare Technology Office Marine Corps Systems Command Quantico, VA 22134		10. SPONSORING/MONITORING AGENCY REPORT NUMBER	
11. SUPPLEMENTARY NOTES			
12a. DISTRIBUTION/AVAILABILITY STATEMENT  Approved for public release; distribution is unlimited.		12b. DISTRIBUTION CODE	
13. ABSTRACT (Maximum 200 words)  The Wideband Antenna Feasibility Study is an ongoing effort originally funded through the Amphibious Warfare Technology (AWT) Office at Marine Corps Systems Command (MARCORSYSCOM). This report gives a technical account of the achievements made during Fiscal Year 1999 (FY 1999). It describes the technical considerations addressed and the basis upon which the concept and specific designs were chosen. Theoretically derived predictions as well as test results are included with a concluding analysis and recommendations.			
14. SUBJECT TERMS Mission Area: Command, Control, Communications decision support tactical command center amphibious assault RF antenna			15. NUMBER OF PAGES  56
			16. PRICE CODE
17. SECURITY CLASSIFICATION OF REPORT  UNCLASSIFIED	18. SECURITY CLASSIFICATION OF THIS PAGE  UNCLASSIFIED	19. SECURITY CLASSIFICATION OF ABSTRACT  UNCLASSIFIED	20. LIMITATION OF ABSTRACT  SAME AS REPORT



21a. NAME OF RESPONSIBLE INDIVIDUAL  R. C. Adams	21b. TELEPHONE <i>(include Area Code)</i>  (619) 553-4313 e-mail: radams@spawar.navy.mil	21c. OFFICE SYMBOL  Code D855

## INITIAL DISTRIBUTION

D0012	Patent Counsel	(1)
D0271	Archive/Stock	(6)
D0274	Library	(2)
D027	M. E. Cathcart	(1)
D0271	D. Richter	(1)
D12	LCDR P. C. Haglind	(2)
D12	USMC Office	(5)
D653	CW03 F. V. Canez	(1)
D841	R. C. North	(2)
D855	R. C. Adams	(4)
D855	LCDR H. Pace, Jr.	(2)

Defense Technical Information Center  
Fort Belvoir, VA 22060-6218 (4)

SSC San Diego Liaison Office  
Arlington, VA 22202-4804

Center for Naval Analyses  
Alexandria, VA 22302-0268

Navy Acquisition, Research and  
Development Information Center  
Arlington, VA 22202-3734

Government Industry Data Exchange  
Program Operations Center  
Corona, CA 91718-8000

Naval Postgraduate School  
Monterey, CA 93943-5001 (6)

Office of Naval Research  
Arlington, VA 22217-5660 (5)

Space and Naval Warfare Systems Command  
San Diego, CA 92110-3127

Marine Corps Warfighting Lab  
Quantico, VA 22134

Marine Corps Systems Command  
Quantico, VA 22134-5080 (3)